

Quantification of a silver contrast agent in dual-energy breast x-ray imaging

Roshan Karunamuni, Andrew D.A. Maidment

Department of Radiology, University of Pennsylvania, Philadelphia, PA 19104

ABSTRACT

Dual-energy (DE) breast x-ray imaging involves acquiring images using a low- and high-energy x-ray spectral pair. These images are then subtracted with a weighting factor that eliminates the soft-tissue signal variation present in the breast leaving only contrast that is attributed to an exogenous imaging agent. We have previously demonstrated the potential for silver (Ag) as a contrast material for DE breast imaging. Theoretical analysis shows that silver can provide better contrast to clinically-used iodine. Here, we present the subtraction method developed to eliminate the contrast between adipose and glandular tissue; the two major component materials in the breast. The weighting factor is calculated from the attenuation coefficients of the two tissue types and varies between values of 0 and 1 for the energy combinations studied. A spectral search was performed to identify the set of clinically-feasible imaging parameters that will optimize the contrast of silver using our subtraction technique. The subtraction methodology was tested experimentally using step-phantoms and demonstrated that we are able to a) nullify the soft-tissue contrast that arises from differences in glandularity, and b) preserve an image contrast for silver that is independent of the underlying soft-tissue composition. By applying the DE subtraction proposed, a silver-based agent will outperform an iodinated contrast agent on a commercially-available CEDE breast x-ray imaging system.

Keywords: breast cancer imaging, dual-energy subtraction, contrast agents, silver

1. INTRODUCTION

Contrast-enhanced dual-energy (CEDE) breast x-ray imaging encompasses an emerging group of modalities that aim to provide quantitative functional information together with high-resolution anatomical data. The unique combination of information in a single imaging procedure represents a powerful breast imaging tool for morphological and vascular characterization of breast lesions [1-4]. DE imaging is used to increase the contrast of radiographic imaging agents by suppressing the anatomical signal variation in the body. In the breast, this involves the suppression of the signal variation that arises from differences in soft tissue (adipose and glandular) composition across the image. By reducing the effect of this soft tissue noise, it is then possible to segment and quantify the signal from an exogenous imaging agent. In CEDE imaging, two distinct energy windows (low- and high-) are used to quantify the variation in attenuation with energy. By employing a contrast agent whose linear attenuation k-edge lies within the energy ranges used, it is possible to separate its signal from the surrounding tissue.

Traditionally, CEDE breast imaging has been employed with an iodinated contrast agent. These agents do, however, possess several limitations that have fueled the research for improved imaging agents [5]. The non-specific nature of the contrast agent results in random vascular permeation, and their relatively low molecular weight facilitates rapid renal clearance. Because these agents lack an appropriate layer of surface biomolecules to prevent the non-specific binding of blood serum proteins, the percentage of the injected dose that reaches the tumor site is low. Perhaps most importantly, iodinated contrast agents were designed for radiographic imaging procedures at much higher x-ray energy ranges than those used in breast imaging. Thus, a more radiographically-suited breast imaging agent is proposed.

We have previously demonstrated the potential for silver as a contrast material for DE breast imaging. Silver represents an attractive base material due to the central location of its k-edge (25.5 keV [6]) in the mammographic clinical energy range. Silver filtration is commonplace in the clinic today, and should allow us to position spectra on either-side of the k-edge. There already exists a significant amount of literature on the development of silver nanoparticles which can be used in the synthesis of a silver-based imaging agent [7-8]. The purpose of this work is to explore, in detail, the DE subtraction methodology needed to remove soft-tissue contrast while maintaining the signal from a silver imaging agent.

2. METHOD

2.1 Imaging Framework

The signal intensity from either the low- or high- energy image can be expressed in terms of the various attenuation coefficients and corresponding thicknesses of materials present in the beam path. In the simplistic case of a monoenergetic x-ray source, these signal intensities can be formulated using the Beer-Lambert law as:

$$\ln(I) = \ln(I_0) + (-\sum \mu t), \quad (1)$$

where I_0 is the initial photon fluence, μ is the linear attenuation coefficient, t is the thickness of the material. In the case of dual-energy breast x-ray imaging, the principal materials that contribute to the attenuation of the x-ray photons are adipose (a), glandular (g) and contrast agent (c). Thus Equation 1, can be rewritten with these three materials for both low-(L) and high-(H) energy photons.

$$\ln(I^L) = \ln(I_0^L) + (-\mu_a^L t_a - \mu_g^L t_g - \mu_c^L t_c) \quad (2)$$

$$\ln(I^H) = \ln(I_0^H) + (-\mu_a^H t_a - \mu_g^H t_g - \mu_c^H t_c). \quad (3)$$

If we then assume that the total thickness of tissue, t can be expressed as the sum of adipose and glandular thicknesses:

$$t = t_a + t_g, \quad (4)$$

we can substitute out t_a in Equations 2 and 3. Thus the signal intensity at each energy level can be described in terms of the total thickness of tissue, the amount of glandular tissue, and the amount of contrast material:

$$\ln(I^L) = \ln(I_0^L) - \mu_a^L t + t_g(\mu_a^L - \mu_g^L) - \mu_c^L t_c \quad (5)$$

$$\ln(I^H) = \ln(I_0^H) - \mu_a^H t + t_g(\mu_a^H - \mu_g^H) - \mu_c^H t_c \quad (6)$$

The DE signal intensity (SI_{DE}) can be expressed as a weighted (W) subtraction between the high- and low- energy signal intensities.

$$SI^{DE} = \ln(I_0^H) - W \times \ln(I_0^L) + t \times [-\mu_a^H + W \times \mu_a^L] + t_g \times [(\mu_a^H - \mu_g^H) - W \times (\mu_a^L - \mu_g^L)] + t_c \times [-\mu_c^H + W \times \mu_c^L] \quad (7)$$

SI^{DE} can be broken down into three major components. The first component, $\ln(I_0^H) - W \times \ln(I_0^L) + t \times [-\mu_a^H + W \times \mu_a^L]$, is a combination of the initial photon fluence and total thickness of the breast. This component can be assumed to be constant across the image and thus provides an offset to SI^{DE} . The second component, $t_g \times [(\mu_a^H - \mu_g^H) - W \times (\mu_a^L - \mu_g^L)]$, describes the relationship between SI^{DE} and the amount of glandular tissue in the beam. By choosing W as:

$$W = \frac{\mu_a^H - \mu_g^H}{\mu_a^L - \mu_g^L}, \quad (8)$$

we can eliminate this dependence. Thus the only remaining term that varies across the image is the third component $t_c[-\mu_c^H + w \times \mu_c^L]$. This component quantifies the linear relationship between SI^{DE} and the thickness of contrast material. The contrast, S_C , can be defined as the change in SI_{DE} with respect to t_c :

$$\frac{d(SI^{DE})}{d(t)} = S_C = -\mu_c^H + \frac{\mu_a^H - \mu_g^H}{\mu_a^L - \mu_g^L} \times \mu_c^L, \quad (9)$$

2.2 Monoenergetic Simulation Testing

The subtraction method was tested using a computer-simulated, monoenergetic x-ray acquisition. Photons of a single energy are passed through a 5 cm step-wedge phantom that consists of sections ranging from 0 to 100% glandular, in 25% increments. The photons are then recorded on an ideal, energy-integrating detector in the absence of scatter or glare. A section of the phantom is replaced with breast material that has been mixed with a certain

concentration of silver. In this manner, simulated high- and low- energy images were acquired and then subtracted using the weighting factors calculated in (8).

2.3 Spectral Optimization

A spectral simulation search was performed to identify the combination of clinically-feasible imaging parameters that maximized contrast for Ag. The parameters chosen for the search are limited to those that are experimentally feasible on the Hologic CEDE Dimensions system.

Table 1. Parameters used for the spectral search.

Parameter	Values
Target	Tungsten
Low Energy kVp	23 to 32
High Energy kVp	36 to 49
Filter Materials	Low Energy: Ag, Rh, Al High Energy: Cu
	All spectra were pre-filtered with 50 cm of air and 0.7 mm Be
Detector	Si, energy-integrating

Polyenergetic tungsten spectra were simulated using Boone's interpolation method and filtered using the Beer-Lambert law. The signal intensity recorded on the detector was calculated as:

$$SI = \sum_{E=1}^{kVp} N_E \times F_m \times F_d \times E \quad (10)$$

where:

N_E is the number of photons at the energy E, calculated using Boone's method [9].

$F_m = e^{\Sigma(-\mu t)}$ for all materials present in the beam path

$F_d = (1 - e^{-(\mu t)_d})$ for the detector (d)

The standard deviation, σ , of the signal intensity was calculated as:

$$S\sigma = SI^{0.46} \quad (11)$$

The coefficient of 0.46 was obtained from Marshall *et al.* where the noise in a Hologic Selenia system was characterized. A low- and high- energy spectral pair were then passed through either a block of 100% adipose or 100% glandular tissue. W can be calculated using signal intensities (SI) as:

$$W = \frac{\ln(SI_a^H) - \ln(SI_g^H)}{\ln(SI_a^L) - \ln(SI_g^L)} \quad (12)$$

Equation 12 can be thought of as the equivalent of Equation 8 for a polyenergetic spectra. The spectral pair used for the calculation of W was then instead passed through a block with a 50% glandular fraction. SI^{DE} was calculated in the presence (SI_{Ag}^{DE}) and absence (SI_{bkg}^{DE}) of a silver contrast agent at a concentration of 1 mg/cm². The signal difference to noise ratio (SDNR) was chosen as the figure of merit to be maximized in the optimization, and was calculated as:

$$SDNR = \frac{SI_{Ag}^{DE} - SI_{bkg}^{DE}}{\sigma_{bkg}^{DE}} \quad (13)$$

where:

$$\sigma^{DE} = \sqrt{\sigma^{2H} + W^2 \times \sigma^{2L} - 2 \times W \times cov(\ln(SI_{bkg}^H), \ln(SI_{bkg}^L))} \quad (14)$$

The covariance term was assumed to be a constant and determined experimentally by obtaining a DE image set of a plain sheet of acrylic, and then calculating the correlation between the signals in a fixed region of interest.

To ensure that the results would produce an optimization point that was clinically feasible, several constraints were applied to the simulation algorithm:

- The total effective dose to the breast was set at 2.4 mGy. However, the manner in which this dose was distributed between the low- and high- energy spectra was allowed to vary. The mean glandular dose to the breast for a given spectrum was calculated using Hendee [10] and Dance [11].
- The mAs required to achieve the desired dose was not allowed to exceed 200 mAs. The required mAs for a given dose was estimated using experimentally-obtained tube output data.
- A minimum threshold detector signal intensity was set.

2.4 Spectral Optimization Validation

A 4cm step phantom was imaged on the Hologic clinical CEDE Dimensions system. A silver foil, measuring 50 μm in thickness, was taped on top of the phantom to mimic an embedded concentration of 25 mg/cm^2 of Ag contrast agent. The phantom was imaged at the optimal conditions found in the previous section as well as other non-optimal combinations of parameters. The low- and high- energy images were then subtracted using the appropriate weighting factors to eliminate the glandular dependence. $SDNR$ was then calculated for each of the DE images. The experimental and simulated values of W and $SDNR$ were compared to validate the simulation algorithm.

3. RESULTS

3.1 Imaging Framework

W (see Figure 1) and S_C of silver (see Figure 2) were calculated for energy combinations between 20 and 50 keV. W was found to have values ranging between 0 and 1 – this is to be expected as the difference in mass attenuation coefficients of adipose and glandular tissue decreases as the energy increases. W tends towards 1 along the diagonal of the plot, for the case where the low and high energy are equal, and is smallest when the low- and high- energies are furthest apart.

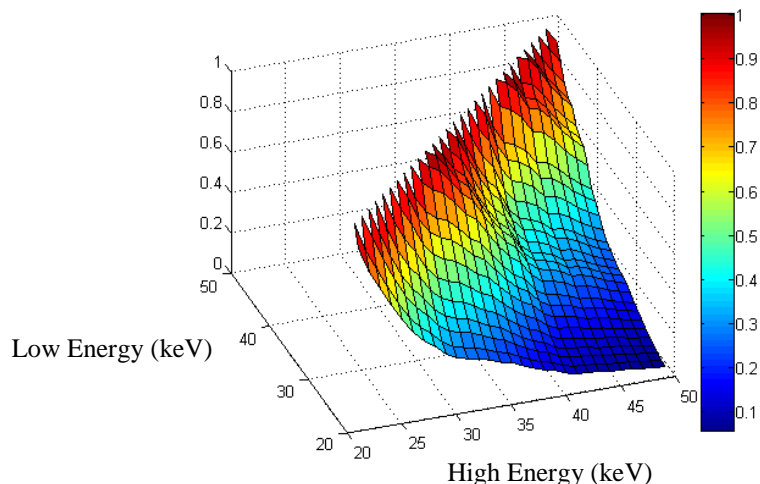


Figure 1. W calculated for energy combinations ranging from 20 to 50 keV. Values ranged from 0 to 1.

As expected, S_C is only significantly greater than zero for energy pairs that bracket the k-edge. The maximum contrast, however, does not occur directly above and below the k-edge but at (21,26) keV. This is due to the effect that the weighting factor, and consequently the attenuation coefficients of adipose and glandular tissue, have on S_C .

Similarly, S_C was calculated for iodine, and plotted in Figure 3. The maximum achievable contrast when using iodine is 33% lower than that of silver.

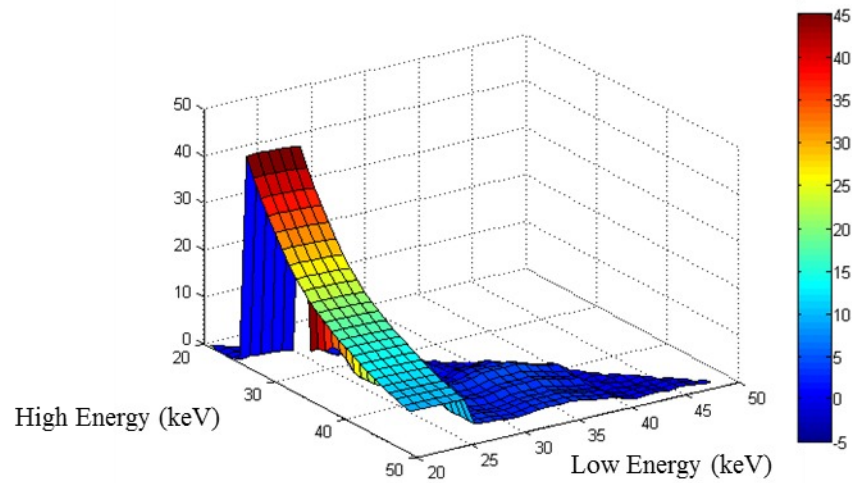


Figure 2. S_C calculated for silver at energy pairs between 20 and 50 keV. The maximum contrast of 45 a.u. occurs at a low energy of 21 keV, and a high energy of 26 keV.

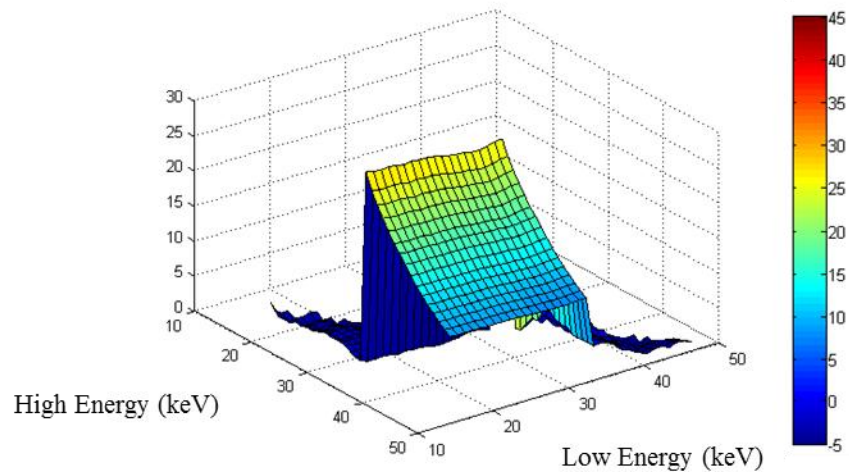


Figure 3. S_C calculated for iodine at energy pairs between 15 and 50 keV. The maximum achievable contrast is 33% lower than that of silver.

3.2 Monoenergetic Simulations

Figure 4 shows the simulated low- and high- energy images that are obtained using an energy pair of (21,26) keV. Each of the single energy images demonstrates a strong SI-dependence on the glandular fraction of the underlying tissue. The section of the phantom that contains Ag, consists of a singular concentration of the element, but results in a gradient of signal intensities because of the underlying variations in soft-tissue composition. By subtracting these single-energy images using W calculated for that energy pair, the DE image shown on the right was obtained.

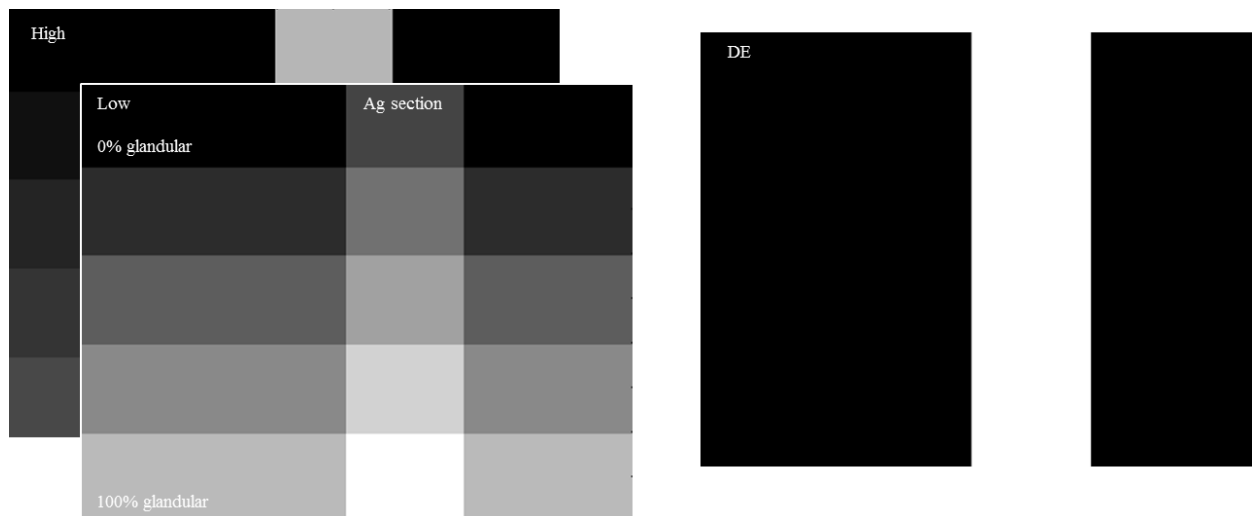


Figure 4. High (26 keV)- and Low (21 keV)- energy images of a step phantom with an section of embedded Ag. The images are subtracted using the pre-calculated weighting factor to yield the DE image shown on the right.

3.3 Spectral Optimization and Validation

Five spectral pairs, including the optimization maximum, were chosen to validate the simulation results (see Table 2). Figure 5 shows the experimentally-determined W plotted against the simulated values. The two sets of data are shown to be highly correlated, with the experimental values assuming a scalar multiple of the simulated data. This scalar is due to the manner in which the Hologic CEDE converts the total number of x-ray photons into digital values.

The $SDNR$ simulated for each of these spectra was compared to the experimentally-obtained values and plotted in Figure 6. The two sets of data are found to be correlated with a coefficient of determination, R^2 , of 0.9407. Spectral Pair 1 was identified as the optimization maximum in the simulation algorithm, and also showed the maximum experimental $SDNR$. An identical simulation algorithm was run for an iodine contrast agent, and the maximum $SDNR$ was calculated to be 15% lower than that of Spectral Pair 1.

Low- and high-energy images, along with the DE subtraction, are shown in Figure 7 for the step phantom imaged using Spectral Pair 1. A line segment (shown in blue), spanning all glandular fractions, was placed in each of the DE, low-, and high-energy images. The mean (γ) and standard deviation (σ) of the SI of the pixels in a given image were then calculated, and the coefficient of variation c_v of the background SI was computed as:

$$c_v = \frac{\gamma}{\sigma} \quad (15)$$

Similarly, six square regions of interest (Figure 7, 5 in red over the silver, 1 in green over the background) were used to calculate the $SDNR$ at five locations of the phantom marked with red squares. c_v of the $SDNR$ and background SI are tabulated in Table 3. In each case, c_v is smallest in the DE image.

Table 2. Spectra chosen for validation of optimization results. The table includes the high- and low- energy kVp and filter choice along with the dose fraction to the low-energy spectrum. The optimization maximum is highlighted in gray.

Spectral Pair	High Energy	Low Energy	Dose fraction to LE
1	46 - Cu	27 - Rh	0.5
2	49 - Cu	27 - Al	0.6
3	49 - Cu	34 - Ag	0.6
4	49 - Cu	33 - Rh	0.8
5	40 - Cu	35 - Al	0.8

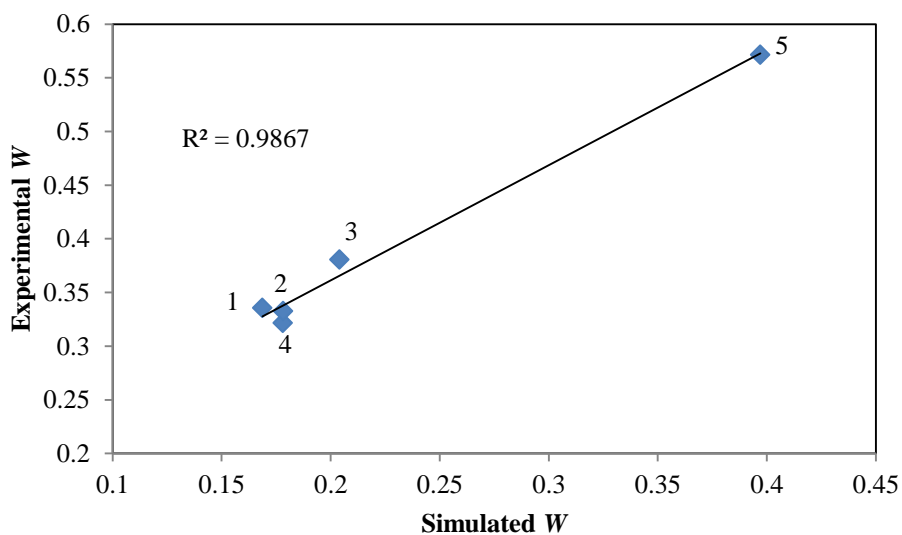


Figure 5. The experimental and simulated values of *W* show excellent agreement.

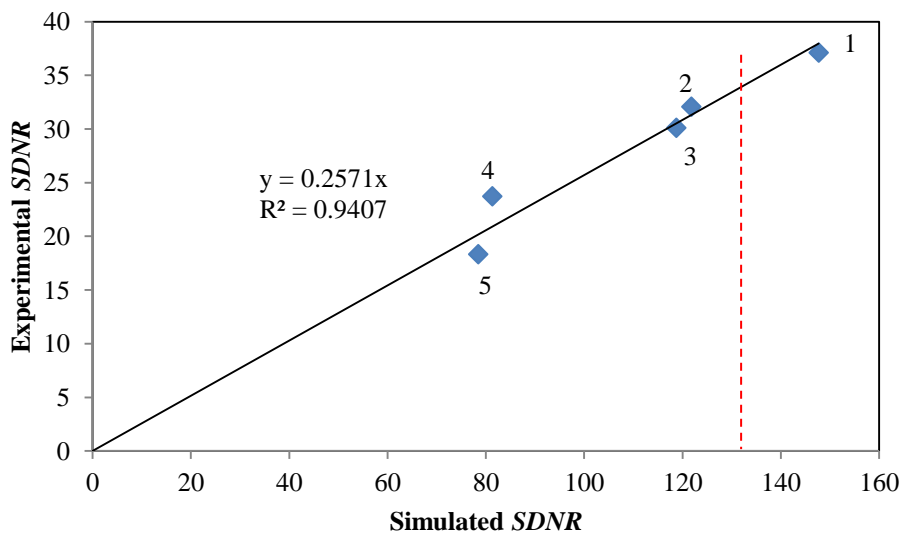


Figure 6. Correlation between simulated and experimental *SDNR* values. The data shows excellent agreement between the simulated and experimentally-obtained values, with the optimization point providing the maximum in both. The red dashed line indicates the maximum simulated *SDNR* for iodine, calculated under the same constraints.

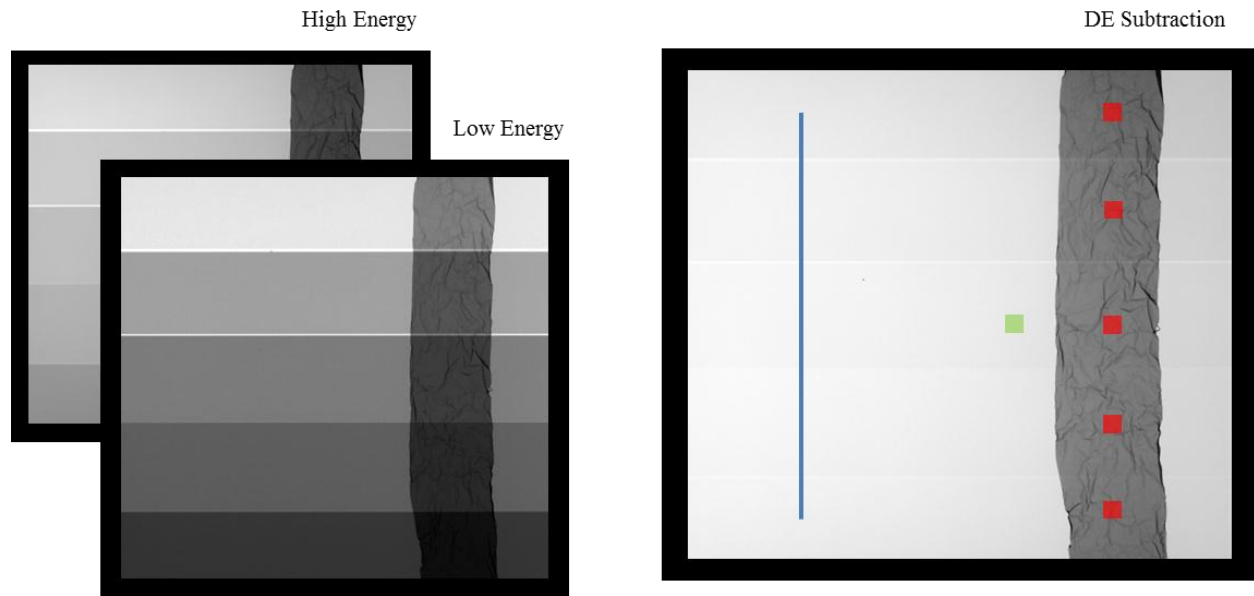


Figure 7. Low- and high-energy images along with the DE subtraction of a 4 cm step phantom with a silver foil emulating an areal concentration of 25 mg/cm². The artifacts present in the image of the foil arise from physical imperfections in the material.

Table 3. Coefficient of variation, c_v , for the background SI and SDNR in each of the DE, low- and high-energy images. For both cases, c_v of the DE image is the smallest.

c_v	DE	Low-Energy	High Energy
Background SI	0.072	0.71	0.12
SDNR	0.0036	0.28	0.0095

4. DISCUSSION AND CONCLUSIONS

The goal of this study was to develop a DE subtraction method for silver that would remove soft tissue signal variation while preserving the contrast from the imaging agent. A framework was developed in Equations 1 through 9 using a monoenergetic analysis of the signal intensities obtained from a low- and high-energy acquisition. The weighting factor, W , that is needed to be applied to the low-energy image in the DE subtraction is formulated in Equation 8. W is independent of the choice of contrast material, and solely depends on the low- and high-energy attenuation coefficients of adipose and glandular tissue. W is plotted in Figure 1 for combinations of energies ranging from 20 to 50 keV. W assumes values between 0 (when the low- and high-energies are furthest apart) and 1 (for the trivial case when the low- and high-energy are the same).

The theoretical DE contrast, S_C , observed from an imaging agent is formulated in Equation 9. S_C is plotted in Figures 2 and 3 for silver and iodine, respectively. For both materials, S_C is only significantly greater than zero at energy pairs that bracket the k-edge of the material (25 keV – silver, 33 keV – iodine). Interestingly, the maximum value of S_C does not occur directly above and below the k-edge where the difference between the attenuation coefficient is the greatest. Instead, S_C of silver is maximum at an energy pair of (LE,HE) = (21,26) keV. This is due to the effect that the weighting factor, and consequently the attenuation coefficients of adipose and glandular tissue, have on S_C . The maximum achievable contrast of iodine is 33% lower than that of silver, implying that a silver contrast agent would be better suited as a DE imaging agent in the mammographic energy range.

A monoenergetic image acquisition was then simulated using the energy pair (21, 26) keV that maximized S_C of silver. Figure 4 shows the DE, low-, and high-energy images that were obtained. The DE image demonstrates two important features that are critical to CEDE imaging. First, the soft-tissue contrast has been nullified. The

background signal has been reduced to a single value that is independent of the glandular percentage. Second, the contrast in the silver is maintained and independent of the underlying soft-tissue composition

A polyenergetic simulation was then performed to identify the set of clinically-feasible imaging parameters that optimized the contrast for silver. In this particular study, the optimization was performed for a Hologic CE-DBT system; parameters listed in Table 1. The simulation was further constrained to ensure that the total mean glandular dose to the breast was 2.4 mGy. The optimal imaging technique consisted of a 46 kVp high-energy beam and a 27 kVp low-energy beam with rhodium filtration, at a dose distribution of 50:50. This low-energy technique is a classic example of an anatomical image that is obtained in the clinic today. In the case of an iodine agent, this low-energy kVp would need to be higher to accommodate for the higher k-edge of iodine. This further supports our hypothesis that silver is a superior DE imaging agent to iodine in the mammographic energy range.

Table 2 shows the four additional spectral pairs that were chosen to test the validity of the simulation algorithm identifying Spectral Pair 1 as the optimization point. The experimental values of W for each of the spectral pairs was shown to correlate well with the simulated numbers as shown in Figure 5. The inability to perfectly estimate W arises from the inability to exactly simulate the conversion of x-ray photons absorbed in the detector to digital units. As shown in Figure 6, the experimentally-determined SDNR was shown to highly correlated with the simulated values. Spectral Pair 1 proved to maximize the SDNR in both the experiments and simulations. Additionally, the maximum simulated SDNR for an iodine agent is 15% lower than that of Spectral Pair 1, further supporting that silver is a better DE imaging agent in the mammographic energy range.

DE, low-, and high-energy images of the step phantom imaged using Spectral Pair 1 is shown in Figure 7. The coefficient of variation, c_v , of the background SI and the SDNR of the silver at various locations in the phantom are tabulated in Table 3. In both cases, the DE image demonstrates the lowest c_v . This indicates that the DE subtraction succeeded in removing the soft-tissue signal variation present at the single-energy images, as well as maintaining the SDNR of a silver contrast agent regardless of the underlying soft-tissue composition. This work leads us to believe that by applying the DE subtraction proposed, a silver-based agent will outperform an iodinated contrast agent on a commercially-available CEDE breast x-ray imaging system.

5. REFERENCES

1. Carton AK, Ullberg C, Lindman K, Acciavati R, Francke T, Maidment ADA. Optimization of a dual-energy contrast-enhanced technique for a photon-counting digital breast tomosynthesis system: I. A theoretical model. *Med Phys.* 2010 Nov; 37(11): 5896 -5907
2. Carton AK, Ullberg C, Maidment ADA. Optimization of a dual-energy contrast-enhanced technique for a photon-counting digital breast tomosynthesis system: II. An experimental validation. *Med Phys.* 2010 Nov; 37(11):5908-5913
3. Carton AK, Gavenonis S, Currivan JA, Conant E, Schnall MD, Maidment ADA. Dual-energy contrast-enhanced digital breast tomosynthesis – a feasibility study. *British Journal of Radiology.* 2010; 83:344-350
4. Chen SC, Carton AK, Albert M, Conant E, Schnall MD, Maidment ADA. Initial clinical experience with contrast-enhanced digital breast tomosynthesis. *Acad Radiol.* 2007 Feb; 14(2):229-238
5. Hainfeld J, Slatkin DN, Focella TM, Smilowitz HM. Gold particles: a new X-ray contrast agent. *British Journal of Radiology.* 2006 Mar; 79:248-253
6. NIST.gov [homepage on the Internet]. NIST X-ray Transition Energies; 2011 [updated 2011 December 9; cited 2013 Feb 19]. Available from: <http://www.nist.gov/pml/data/xraytrans/index.cfm>
7. Sun Y, Xia Y. Shape-Controlled Synthesis of Gold and Silver Nanoparticles. *Science.* 2002 Dec 13; 298: 2176-2179
8. Wang Y, Zheng Y, Huang CZ, Xia Y. Synthesis of Ag Nanocubes 18 – 32 nm in Edge Length: The Effects of Polyol on Reduction Kinetics, Size Control, and Reproducibility. *JACS.* 2013 Jan 14; 135:1941-1951
9. Boone JM, Fewell TR, Jennings R. Molybdenum, rhodium, and tungsten anode spectral models using interpolating polynomials with application to mammography. *Med Phys.* 1997 Dec; 24(12):1863-1874
10. Hendeel WR, Ritenour ER. *Medical Imaging Physics.* 4th ed. Wiley-Liss (NY); 2002.
11. Dance DR. Monte Carlo calculation of conversion factors for the estimation of mean glandular breast dose. *Phys Med Biol.* 1990; 35(9):1211-1219